

Electronic structures of doped anatase TiO_2 : $\text{Ti}_{1-x}\text{M}_x\text{O}_2$ ($\text{M} = \text{Co}, \text{Mn}, \text{Fe}, \text{Ni}$)

Min Sik Park, S.K. Kwon, and B.I. Min

Department of Physics and Electron Spin Science Center,
Pohang University of Science and Technology, Pohang 790-784, Korea
(March 22, 2024)

We have investigated electronic structures of a room temperature diluted magnetic semiconductor: Co-doped anatase TiO_2 . We have obtained the half-metallic ground state in the local-spin-density approximation (LSDA) but the insulating ground state in the LSDA+U+SO incorporating the spin-orbit interaction. In the stoichiometric case, the low spin state of Co is realized with the substantially large orbital moment. However, in the presence of oxygen vacancies near Co, the spin state of Co becomes intermediate. The ferromagnetism in the metallic and insulating phases are accounted for by the double-exchange-like and the superexchange mechanism, respectively. Further, the magnetic ground states are obtained for Mn and Fe doped TiO_2 , while the paramagnetic ground state for Ni-doped TiO_2 .

PACS numbers: 75.50.Pp, 71.22.+i, 75.50.Dd

Diluted magnetic semiconductors (DMSS) have been studied extensively for last decades, because of their potential usages of both charge and spin degrees of freedom of carriers in the electronic devices, namely the spintronics. There have been trials based on two types of DMSS families: II-VI such as Mn-doped CdTe and ZnSe [1], and III-V such as Mn-doped GaAs [2]. Especially, the latter attracts great attention, because it becomes a ferromagnetic (FM) DMSS having the Curie temperature $T_C \sim 110\text{K}$. Motivated by the above FM DMSS, recent research effort has been focused on developing new FM semiconductors operating at room temperature [3,4]. It has been reported that the FM DMSS are realized in other types of systems too [5-7].

Matsumoto et al. [6] fabricated Co-doped anatase TiO_2 thin film samples, $\text{Ti}_{1-x}\text{Co}_x\text{O}_2$, using the combinatorial pulsed-laser-deposition (PLD) molecular beam epitaxy (MBE) technique. A sizable amount of Co, up to $x = 0.08$, is soluble in anatase TiO_2 . Using the scanning SQUID microscope, they observed the magnetic domain structures in Co-doped films characteristic of the FM long range ordering. The measured saturated magnetic moment per Co ion was $0.32 \mu_B$ apparently in the low spin state and T_C was estimated to be higher than 400K . This sample is conductive at room temperature, but becomes semiconducting at low temperature. It also exhibits a large positive magnetoresistance of 60% at 2K in a field of 8T . Due to transparent property of the system, it can be used in integrated circuits and storage devices with display units [8].

More recently the Co-doped anatase TiO_2 film grown by the oxygen-plasma-assisted (OPA) MBE was reported by Chambers et al. [9]. They claimed that magnetic properties of the OPA-MBE grown material are better than those of the PLD-MBE grown material because considerably larger saturated magnetic moment of $1.26 \mu_B/\text{Co}$ is observed, which seems to be consistent better with the low spin state of Co. The unquenched orbital moment of Co in the asymmetric crystalline field was ascribed to

the enhanced magnetic moment. The Co L-edge x-ray absorption (XAS) spectrum of Co-doped TiO_2 is similar to that of CoTiO_3 , whereby the formal oxidation state of Co^{2+} has been suggested. They also found that the magnetic and structural properties depend critically on the Co distribution which varies widely with the growth condition.

Hence the magnetic properties of Co-doped anatase TiO_2 are still controversial. To explore these properties, the essential first step is to study the electronic structure of Co-doped anatase TiO_2 . In this study, we have investigated electronic structures of Co-doped anatase TiO_2 : $\text{Ti}_{1-x}\text{Co}_x\text{O}_2$ ($x = 0.0625$ and 0.125) using the linearized muffin-tin orbital (LMTO) band method both in the local-spin-density approximation (LSDA) and the LSDA+U+SO incorporating the Coulomb correlation interaction U and the spin-orbit interaction [10]. For a comparison, we have also investigated electronic structures of other transition metal doped TiO_2 : $\text{Ti}_{1-x}\text{M}_x\text{O}_2$ ($\text{M} = \text{Mn}, \text{Fe}, \text{Ni}$).

TiO_2 has three kinds of structures, rutile, anatase, and brookite. The space group of anatase structure is tetragonal $I4_1/am$. The anatase TiO_2 is composed of stacked edge-sharing octahedrons formed by six O anions. Ti atoms are in the interstitial sites of octahedrons that are distorted with different bond lengths between the apical (1.979 \AA) and the equatorial (1.932 \AA) Ti-O bond and with the Ti-O-Ti angle 156.3° . For $\text{Ti}_{1-x}\text{Co}_x\text{O}_2$ ($x = 0.0625$), we have considered a supercell containing sixteen formula units in the primitive unit cell by replacing one Ti by Co ($\text{Ti}_{15}\text{Co}_1\text{O}_{32}$: $a = b = 7.570$; $c = 9.514 \text{ \AA}$). Sixteen empty spheres are employed in the interstitial sites to enhance the packing ratio for the LMTO band calculation.

We have first calculated the electronic structure of anatase TiO_2 without doping elements. The overall band structure of the present LMTO result is consistent with existing results [11], except that the energy gap is estimated a bit larger, $\sim 4 \text{ eV}$, as compared to the FLAPW

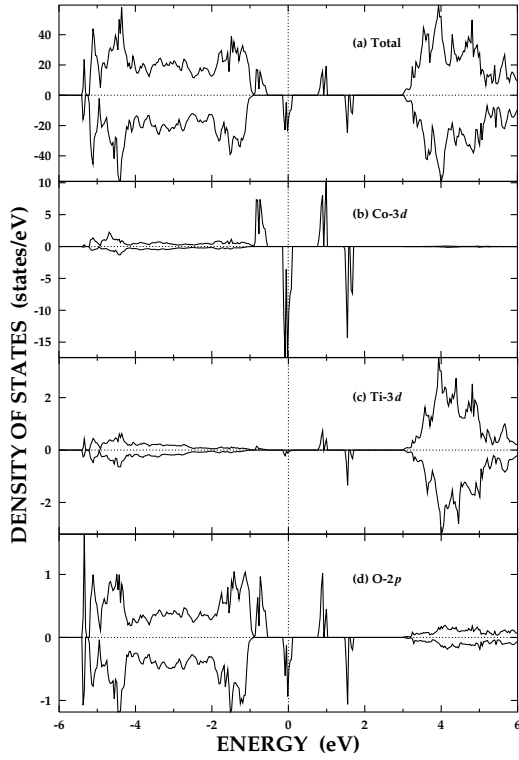


FIG. 1. The LSDA total and PLDOS of $\text{Ti}_{1-x}\text{Co}_x\text{O}_2$ ($x = 0.0625$).

result of ~ 2 eV [11]. Although the present result is closer to the experimental energy gap of 3.2 eV, it is likely that the energy gap is overestimated due to the open structure of anatase TiO_2 and the minimal basis of the LMTO band method. The valence band top and the conduction band bottom correspond to mainly O-2p and Ti-3d states, respectively. The electronic transport and magnetic experiments on anatase TiO_2 indicate peculiar properties, such as shallow donor level and high mobility of the n-type carriers due to intrinsic oxygen stoichiometry [12].

To examine the energetics of $\text{Ti}_{1-x}\text{Co}_x\text{O}_2$ between the FM and antiferromagnetic (AFM) configurations of Co ions, we have performed the LSDA band calculation for anatase $\text{Ti}_{1-x}\text{Co}_x\text{O}_2$ ($x = 0.125$). In this case, there are two Co ions in the unit cell ($\text{Ti}_4\text{Co}_2\text{O}_{32}$) separated by 5.35 Å. In between two Co ions, there are one Ti and two O ions. As a result, we have obtained that the FM phase has half-metallic electronic structure, while the AFM phase has semiconducting electronic structure. Total energies are very close, but the FM phase is lower by 6 mRy than the AFM phase. Hence, in the following discussion, we will consider only the FM configurations of Co ions.

Now, we have performed band calculations for anatase $\text{Ti}_{1-x}\text{Co}_x\text{O}_2$ ($x = 0.0625$). Figure 1 shows the density of states (DOS) obtained from the LSDA band calculation. The energy gap between O-2p and Ti-3d states

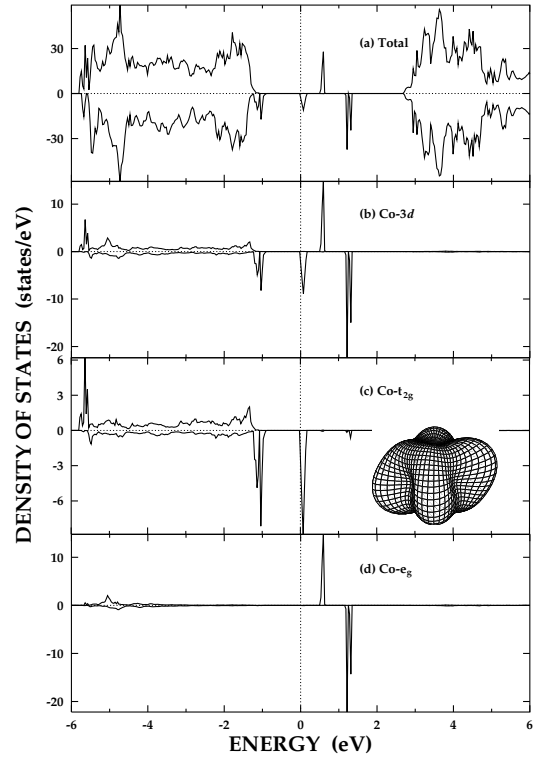


FIG. 2. The LSDA+U+SO total and PLDOS for $\text{Ti}_{1-x}\text{Co}_x\text{O}_2$ ($x = 0.0625$). The angular distribution of occupied Co-3d spin-down states (inset (c)).

is almost unchanged by Co doping and most of Co d states are located in the energy gap region. Noteworthy is the half-metallic nature in this system, reminiscent of the Mn-doped GaAs [13{15], that is, the conduction electrons at the Fermi level E_F are 100% spin-polarized. The carrier types, however, are different between two. Here the Fermi level cuts the Co t_{2g} states, whereas, in Mn-doped GaAs, the Fermi level cuts mainly the As p states since Mn-3d states are located far below E_F . The different carrier types would give rise to the different magnetic mechanisms as discussed below [16]. The crystal field splitting between t_{2g} and e_g state is larger than the exchange splitting between t_{2g} states, suggesting the low spin state of Co. The total spin magnetic moment is $1 \mu_B$, which comes mostly from Co ions. Ignoring the extended Co-d states between ~ 5 and ~ 1 eV, which are hybridized bonding states with O-2p states, the characters of localized d states are mainly t_{2g}^3 spin-up and t_{2g}^2 spin-down states, seemingly corresponding to the ionic valence of Co^{4+} . However, almost two electrons are occupied in the extended Co d states, and so the total occupancy of d states amounts to d^7 .

The half-metallic LSDA result for Co-doped TiO_2 seems to be compatible with the metallic resistivity behavior above 100K. Further, in view of the carrier type of Co-3d, the FM ground state can be understood based on the double-exchange-like mechanism, e.g., the kinetic

energy gain through the hopping of fully spin-polarized carriers in the half-metallic system. This is contrary to the case of Mn-doped GaAs in which As p-hole carriers mediate the RKKY-like exchange interaction. Note, however, that at low temperature the system behaves as an insulator [6]. Since the unfilled t_{2g} states near E_F are very narrow, one can expect that the Coulomb correlation interaction and/or the Jahn-Teller interaction would induce the metal-insulator transition. The Jahn-Teller effect would be relatively weak because the relevant orbitals near E_F are t_{2g} states. Thus we have explored the effect of the Coulomb correlation interaction using the LSDA+U+SO band method. The spin-orbit interaction is taken into account to describe properly atomic-like Co- t_{2g} states.

Indeed, the LSDA+U+SO band calculation with parameter values of $U = 3.0$ eV and $J = 0.87$ eV for Co-3d electrons yields the semiconducting ground state in accord with the experiment. The DOS plot in Fig. 2 shows that the t_{2g} spin-down states are separated by the U effect with the band gap size of 0.8 eV. The total spin magnetic moment of $1 \mu_B$ and the occupancy of d^7 are also obtained by the LSDA+U+SO. In the inset of Fig. 2(c), the angular distribution of occupied Co 3d spin-down states are plotted, based on the orbital occupancies. The main contribution to these states comes from the d_{xy} state mixed partially with d_{yz} and d_{zx} , which is reflected in the shape of the angular distribution. Due to the spin-orbit effect, however, the shape is a bit asymmetric and distorted.

Evidently, atomic-like Co t_{2g} states would yield the unquenched orbital moment. In fact, Co-ion has remarkably large orbital magnetic moment of $0.9 \mu_B$ which is as large as that in CoO ($1.0 \mu_B$) [17]. The large orbital moment arises from occupied t_{2g} spin-down states split by the Coulomb correlation and the spin-orbit interaction (Fig. 2). The orbital moment is polarized in parallel with the spin moment, and so the total magnetic moment amounts to $1.9 \mu_B/\text{Co}$. The large orbital magnetic moment is in agreement with the expectation by Chambers et al. [9], but the total magnetic moment $1.9 \mu_B$ is much larger than their experimental value $1.26 \mu_B$.

As mentioned above, oxygen vacancies are easily formed in the anatase TiO_2 , and so there will also be intrinsic oxygen vacancies in Co-doped TiO_2 . We thus examined the effects of oxygen deficiency in the Co-doped TiO_2 . By removing one oxygen atom in the supercell ($\text{Ti}_{15}\text{Co}_1\text{O}_{31}$), the formal valence of Co becomes Co^{2+} in the ionic picture. We have considered two cases of removing an oxygen atom: (i) from the Ti-contained octahedron, and (ii) from the Co-contained octahedron. For the oxygen vacancy near the Ti site, essentially the same Co-3d projected local density of states (PDOS) are obtained as for the stoichiometric case with the low spin $1.0 \mu_B/\text{Co}$ and the orbital magnetic moment $0.9 \mu_B/\text{Co}$, implying that the Co sites are not affected much by the vacancy [18]. On the other hand, for the oxygen vacancy near the Co site, very different features are revealed:

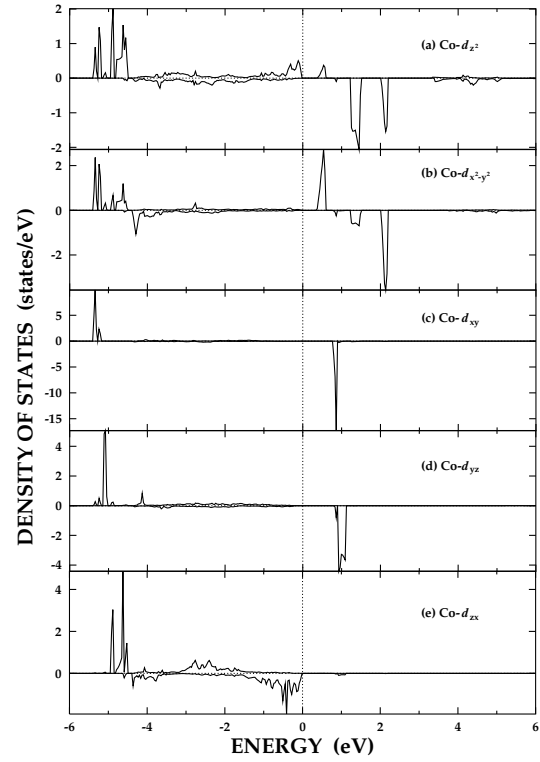


FIG. 3. The LSDA+U+SO Co-PLDOS of oxygen deficient Co-doped TiO_2 ($\text{Ti}_{15}\text{Co}_1\text{O}_{31}$).

the intermediate (close to the high) spin state is realized rather than the low spin state with the spin magnetic moment of $2.53 \mu_B/\text{Co}$. The intermediate spin state in this case results from the reduced crystal field in the pyramidal structure composed of five oxygen anions. Then the d_{z^2} and d_{zx} states become more stabilized than in the case of stoichiometric octahedral structure (see Fig. 3). The configuration of occupied states becomes d^7 with spin-up $t_{2g}^3 d_{z^2}^1$ and extended $d_{x^2-y^2}^1$ bonding states and spin-down e_g^1 and extended t_{2g}^{1+} (mainly d_{zx}) bonding states. Due to decreased t_{2g} characters near E_F , the orbital magnetic moment is reduced to $0.28 \mu_B$. Comparing the total energies between above two cases, the oxygen vacancy near the Ti site is more stable than the oxygen vacancy near the Co site. Therefore oxygen vacancies tend to be formed mostly in the Ti-contained octahedrons without affecting the Co spin state. However, the possible oxygen vacancies near Co-sites formed during the non-equilibrium MBE growth would influence drastically the magnetic properties in Co-doped TiO_2 . This explains the observation that the magnetic properties depend critically on the film growth condition.

For comparison, we have also examined electronic structures of other transition metal doped anatase TiO_2 : $\text{Ti}_{1-x}\text{M}_x\text{O}_2$ ($M = \text{Mn, Fe, Ni}$) for $x = 0.0625$. The same U and J parameters were employed for Mn and Fe 3d electrons. Figure 4 shows that Ni-doped TiO_2 has the paramagnetic ground state, whereas, Mn and Fe doped

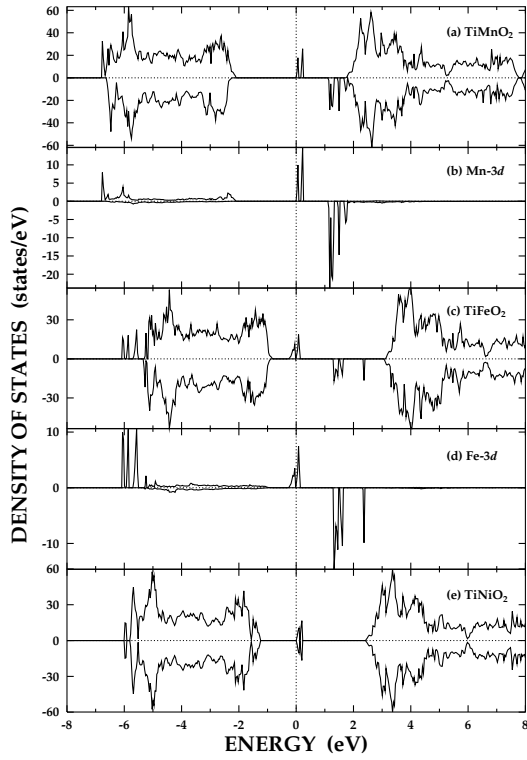


FIG. 4. The LSDA+U DOS of Mn, Fe-doped DOS, and the LSDA DOS of Ni-doped TiO_2 ($x = 0.0625$).

systems have the magnetic ground states with local magnetic moments of 3.0 and 3.7 μ_B , respectively. Ignoring the extended bonding d states, the apparent nominal valences look like Mn^{4+} (d^3) and Fe^{4+} (d^4). Including the extended states, however, the electron configuration for the Mn-doped case becomes d^5 with spin-up $t_{2g}^3 e_g^1$ states and spin-down bonding $t_{2g} e_g^1$ states. Likewise, for the Fe-doped case, the electron configuration becomes d^6 with spin-up $t_{2g}^3 e_g^2$ states and spin-down bonding $t_{2g} e_g^1$ states. Therefore, for both cases, the intermediate close to the high spin states are realized even without oxygen defects.

No evidence of FM behavior has been observed in Mn or Fe-doped TiO_2 in yet. The different magnetic natures in these systems are presumably due to their different electronic structures. Note that the characters of unoccupied states near E_F are different: t_{2g} for the Co-doped TiO_2 (Fig. 2), whereas e_g for the Mn and Fe-doped TiO_2 . For Mn-doped case, even the LSDA yields the insulating electronic structure, and so, by considering only the localized states, the superexchange via occupied Mn(t_{2g})-O(p)-Mn(t_{2g}) orbitals would lead to the nearest neighbor AFM interaction. On the other hand, for Fe-doped case, the LSDA yields the half-metallic electronic structure, as for Co-doped case. The Jahn-Teller effects would be more operative in this case because of the e_g characters near E_F , which will drive the structural distortion and the concomitant metal-insulator transition.

Then the AFM phase is more likely to be stabilized. In contrast, the Co-doped TiO_2 even in its insulating phase would have the nearest neighbor FM superexchange interaction via Co(t_{2g})-O(p)-Co(t_{2g}) kinetic-exchange energy gain. Therefore, the FM phases in the metallic and insulating states are accounted for by the double-exchange-like and the superexchange mechanism, respectively. In reality, however, the situation may not be that simple, since there could be some effects of extra-carriers originating from the intrinsic or extrinsic O-vacancies. The present study serves to provide basic band structure information for understanding the magnetic mechanism in these systems.

In conclusion, the LSDA yields the half-metallic ground state for Co-doped TiO_2 with the carrier type of mainly Co 3d states. In contrast, the LSDA+U+SO yields the insulating ground state and the low spin state with 1 μ_B spin moment and 0.9 μ_B orbital moment per Co ion. The possible oxygen vacancies near Co sites substantially affect the magnetic properties: the intermediate spin state of Co with 2.53 μ_B spin moment is realized and the orbital moment is reduced to 0.28 μ_B . We have also found that Mn and Fe-doped TiO_2 have the magnetic ground states, while Ni-doped TiO_2 has the paramagnetic ground state.

Acknowledgments This work was supported by the KOSEF through the eSSC at POSTECH and in part by the BK21 Project. Helpful discussions with J.-H. Park and Y.-H. Jeong are greatly appreciated.

-
- [1] J.K. Furdyna and J. Kossut, *DMSS, 25 of Semiconductor and Semimetals Academic Press, New York*, (1988).
 - [2] H. Ohno et al., *Appl. Phys. Lett.* 69, 363 (1996).
 - [3] T. Dietl et al., *Science* 287, 1019 (2000).
 - [4] K. Sato and H. K. Yoshida, *Jpn. J. Appl. Phys.* 39, L555 (2000).
 - [5] G. A. Medvedkin et al., *Jpn. J. Appl. Phys.* 39, L949 (2000).
 - [6] Y. Matsumoto et al., *Science* 291, 854 (2001).
 - [7] K. Ando et al., *Appl. Phys. Lett.* 78, 2700 (2001); K. Ueda, H. Tabata, and T. Kawai, *ibid* 79, 988 (2001).
 - [8] H. Ohno, *Science* 291, 840 (2001).
 - [9] S. A. Chambers et al., *Appl. Phys. Lett.* 79, 3467 (2001).
 - [10] S. K. Kwon and B. I. Min, *Phys. Rev. Lett.* 84, 3970 (2000).
 - [11] R. Sahiet al., *Phys. Rev. B* 61, 7459 (2000); and references therein.
 - [12] L. Forro et al., *J. Appl. Phys.* 75, 633 (1994).
 - [13] M. Shirai et al., *J. Magn. Magn. Mater.* 177-181, 1383 (1998).
 - [14] H. Akai, *Phys. Rev. Lett.* 81, 3002 (1998).
 - [15] J. H. Park, S. K. Kwon, B. I. Min, *Physica B* 281-282, 703 (2000).
 - [16] P. Kacman, *Semicond. Sci. Technol.* 16, 25 (2001).

- [17] S.K. Kwon and B.I. Min, Phys. Rev. B 62, 73 (2000).
- [18] For the O-vacancy near Ti, vacancy induced impurity states appear just below the conduction band, but the Co PDOS is essentially the same. Half-metallic electronic structures are obtained in the LSDA for both cases of O-vacancies.